Supplementary information

Temperature and locomotion dual self-sensing soft robot based on liquid crystal polymer foams

Shuyun Zhuo, Jie Jiang, Yaru Ma, Yiming Chen, Yue Zhao*

Departement de chimie, University de Sherbrooke, Sherbrooke, Quebec, J1K 2R1 (Canada)

Contents:

Materials

4,4'-Biphenol (Aldrich, 97%), N,N-Dimethylformamide (DMF, Aldrich, 99.8%), potassium carbonate (K_2CO_3, Fisher Scientific, 99%), 6-chloro-1-hexanol (Aldrich, 96%), Potassium iodide (KI, Anachemia, 99%), hydrochloric acid (HCl, Anachemia), chloroform (Fisher Scientific, 99%), p-coumaric acid (Aldrich, 99%), potassium hydroxide (KOH, Anachemia), Ethyl acetate (EtOH, Fisher Scientific, 99%), 6-chloro-1-hexanol (Fisher Scientific, 99%), (±)-Phenylsuccinic acid (PSA) (Aldrich,98%), Zinc acetate ($Zn(Ac)_2$, Aldrich, 98%), Antimony oxide (Sb_2O_3, Fisher Scientific, 99%), 1-butyl-3-methylimidazolium hexafluorophosphate ($BMIMPF_6$, Aldrich, ≥97.0%), carbon black (Fuelcell store, particle size of 30-60 nm, deionized (DI) water.

Method

Synthesis of the liquid crystal polymer (LCP): two monomers used were synthesized as follows through the previously reported method. [1,2]

4,4'-bis(6-hydroxyhexyloxy) biphenyl (BHHBP): 1.62 g of 4,4'-biphenol, 12.3 g of K_2CO_3, 4 g of 6-chloro-1-hexanol, and 0.05 g of KI were dissolved in 300 ml of DMF. The mixture was refluxed in a nitrogen atmosphere for 24 h. After cooling down and filtering the mixture, the residue was poured into 100 mL deionized water and neutralized with HCl. Then, the formed precipitate was washed with 200 ml deionized water three times. Finally, the precipitate was recrystallized from chloroform, and then dried at 80 ^oC under vacuum for 24 h to obtain a white powder product.

4-(6-Hydroxyhexyloxy)cinnamic acid (6HCA): 5.16 g of KOH was dissolved in 14 mL of deionized water and 40 mL EtOH, then 5.0 g of p-Coumaric acid and trace KI were added to the solution. The mixture was refluxed for 10 min and then 5.0 g of 6-chloro-1-hexanol was added followed by a 48-h reflux. The precipitate was poured into 200 mL deionized water and neutralized with HCl, and filtered, the residue was washed with 200 mL of deionized water. The crude product was recrystallized from EtOH/H2O, then dried at 60 °C under vacuum for 24 h to yield a white solid product.

Liquid crystal polymer (LCP): 1.1596 g of BHHBP, 0.5825 g of PSA, 0.2114 g of 6HCA, 0.0039 g of $Zn(Ac)_2$ and 0.0059 g of Sb_2O_3 were put into a 100-mL three-

necked flask. To remove the oxygen in the flask, vacuum pumping and nitrogen protection were processed before reaction. For the reaction, the flask was heated to 180 °C in a silicone oil bath for 1 h, then heated slowly over 1 h to 200 °C and held for 0.5 h. Afterwards, a low vacuum was employed, and the temperature was preserved at 200 °C for another 0.5 h. The temperature was kept at 200 °C with vacuum of 30-50 Pa for 2.5 h. Finally, the polymerization was completed, and the flask was cooled to room temperature under a vacuum.

Preparation of LCP foams: 1 g of LCP and a certain amount of THF (10, 20, 30, 40, 50, and 60 wt%) were well mixed and then placed in an oven at room temperature and under a pressure of -25 kPa for 3 hours. After the THF was fully removed, the LCP foams were ready to use.

Fabrication of LCE foams (LCEF) actuators: Heat the LCPFs to 53 °C and mechanically stretch the samples to 100%, 300% or 500% strain, followed by exposing the samples under strain to UV light (325 nm, 90 mW/cm^2) for 1 hour for photo-crosslinking. Finally heat the samples to the isotropic phase (65 °C) for 1 minute for thermal equilibrium before cooling them to room temperature.

Fabrication of LCEF sensors: Soak the LCEF actuator in 1-butyl-3-methylimidazolium hexafluorophosphate ($BMIMPF_6$) under a pressure of -25 kPa inside an oven for different times (15 min, 1 hour, and 3 hours). To heat the LCPF sensor remotely, 5 wt% of carbon black was added in $BMIMPF_6$ before soaking the LCPF actuator in the same procedure.

Fabrication of LCPF-N sensor, LCE tuber sensor and LCE/IL sensor:

LCPF-N sensor: Soak the LCP foams in 1-butyl-3-methylimidazolium hexafluorophosphate ($BMIMPF_6$) with 5 wt% carbon black at -25 kPa in an oven for 1 hour.

LCE tube sensor: Dissolve LCP in THF and dip coating the solution on a glass rod. After dried, the LCP tube was heated to 53 °C and mechanically stretched to 300% strain, followed by crosslinking under UV light (325 nm, 90 mW/cm^2) for 1 hour and equilibrating at 65 °C for 1 minute. The aligned and crosslinked LCE tube was then filled with $BMIMPF_6$ to form the LCE tube sensor.

LCE/IL sensor: LCP and 30 wt% $BMIMPF_6$ were dissolved in THF and mixed well. Then the solution was dried to remove the THF. The resultant sample was first heated to 53 °C and mechanically stretched to 300% strain, then crosslinked under UV light (325 nm, 90 mW/cm^2) for 1 hour and equilibrated at 65 °C for 1 minute to form the LCE/IL sensor.

Fabrication of LCEF-based robots: Two thin copper wires were connected to the LCEF sensor at two ends, then the LCEF sensor was taped onto a paper arm. A glossy foot and a matte foot were made from glossy and matte paper respectively and glued to the paper arm.

Characterization

Differential scanning calorimeter (DSC): The LCEF samples were measured using a differential scanning calorimeter (DSC, TA) in the temperature range of -20 to 120 °C at a rate of 10 °C/min under protection of nitrogen (flowing rate of 50 ml/min).

Thermogravimetric analysis (TGA): TA Instruments Trios V5.7.2.101 was used to heat LCPF samples from room temperature to 800 °C at a heating rate of 10 °C/min.

Wide-angle X-ray scattering (WAXS): A Bruker AXS Nanostar system was used with a microfocus copper anode, MONTAL OPTICS and a VANTEC 2000 2D detector at 90 mm from the samples. The X-ray wavelength was 0.154 nm, and the azimuthal scans of 360° were recorded at $2\theta = 17–28°$.

Optical microscope and polarizing microscope measurement: The appearance and microstructure of the LCEFs were observed using an optical microscope. The liquid crystal mesogen alignment was observed using a polarizing microscope at 0° and 45°.

Resistance measurement: The electrical resistance changes of all samples were recorded using a Digital Multimeter DMM6500 6 ½ (Tektronix, Inc.).

Temperature measurement: Temperature was recorded by a Fluke infrared thermal imaging camera. The temperature coefficient of resistance was calculated by $TCR= (R_2-R_1)/R_1(T_2-T_1)$.

Porosity and apparent density measurement: Apparent density was calculated by measuring the weight and volume of the samples. To measure the porosity of open cell foams, the LCP foam samples were soaked in DI water and left in an oven at -30 kPa

and room temperature, letting water fill the foams. The weight of the samples before and after soaking in water was recorded as w_D and w_W; the density of DI water and LCP was measured as ρ_w and ρ_M. The porosity of open cell foam samples was calculated by the following equation:

$$\varepsilon = \frac{(w_W - w_D)/\rho_W}{(w_W - w_D)/\rho_W + w_D/\rho_M} \times 100\%$$

For close cell foam samples (LCPF-10), the porosity was calculated using the weight and density of air instead of DI water.

Actuation measurement: To trigger the actuation of all the actuators, direct heating and light were used. For direct heating, samples were placed on a hotplate and the temperature was controlled manually. For light-trigger actuation, a lamp (Flash Torch) was used to irradiate the samples, and the light intensity was measured using a power meter (TURNER, gentec-co Company). The size changes (length and radium) of the samples were recorded by a camera, and the reversible actuation degree (RAD) was calculated using the following formulas: $RAD_L = (L_2-L_1)/L_1 \times 100\%$ and $RAD_R = (R_1-R_2)/R_2 \times 100\%$, where the L_1, L_2 represent the length, R_1, R_2 are the radius of LCPF samples at extraction and extension, respectively.

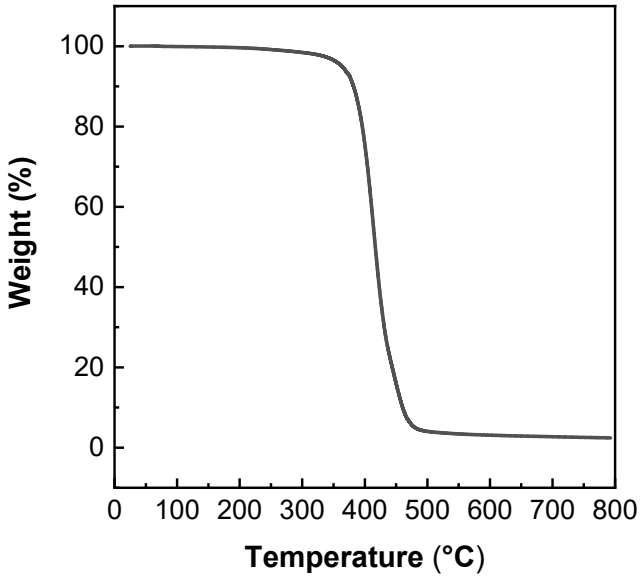

Fig. S1 Thermogravimetric analysis (TGA) of LCPFs.

Fig. S2 Photos of the LCPFs with different shapes and low density, scale bar, 1cm.

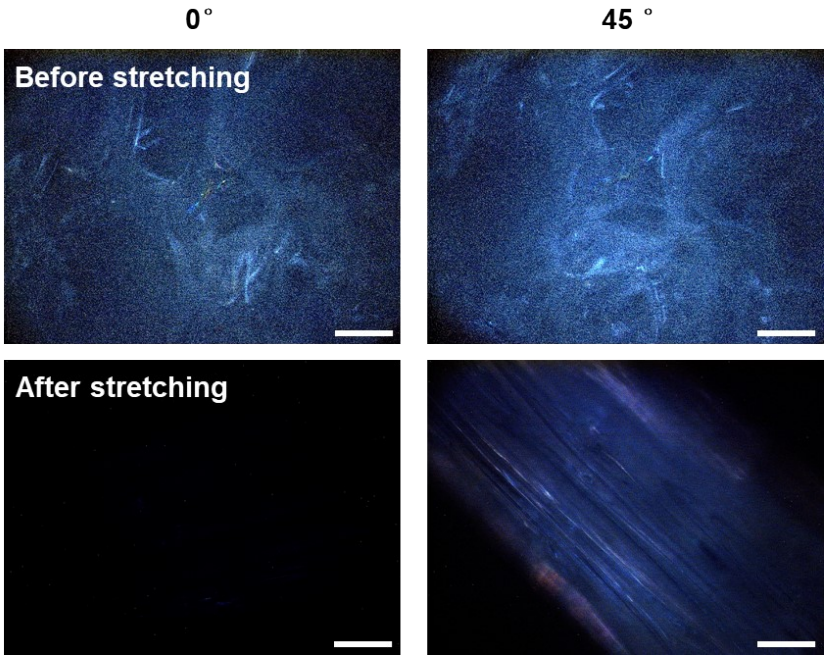

Fig. S3 POM images of the LCP foams before and after stretching. Scale bar, 200 μm.

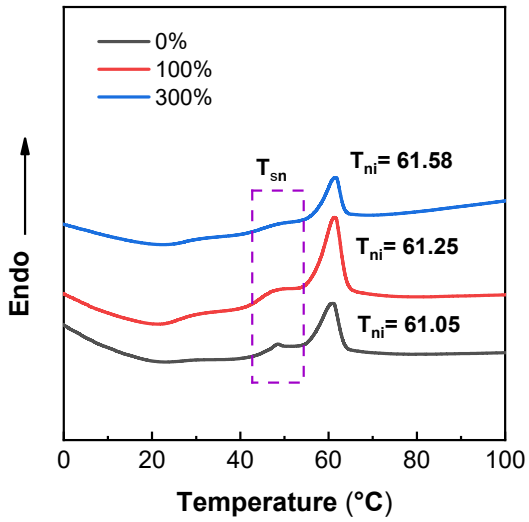

Fig. S4 DSC curves of the liquid crystal elastomer foams (LCEF) stretched to different strains (0%, 100%, and 300%).

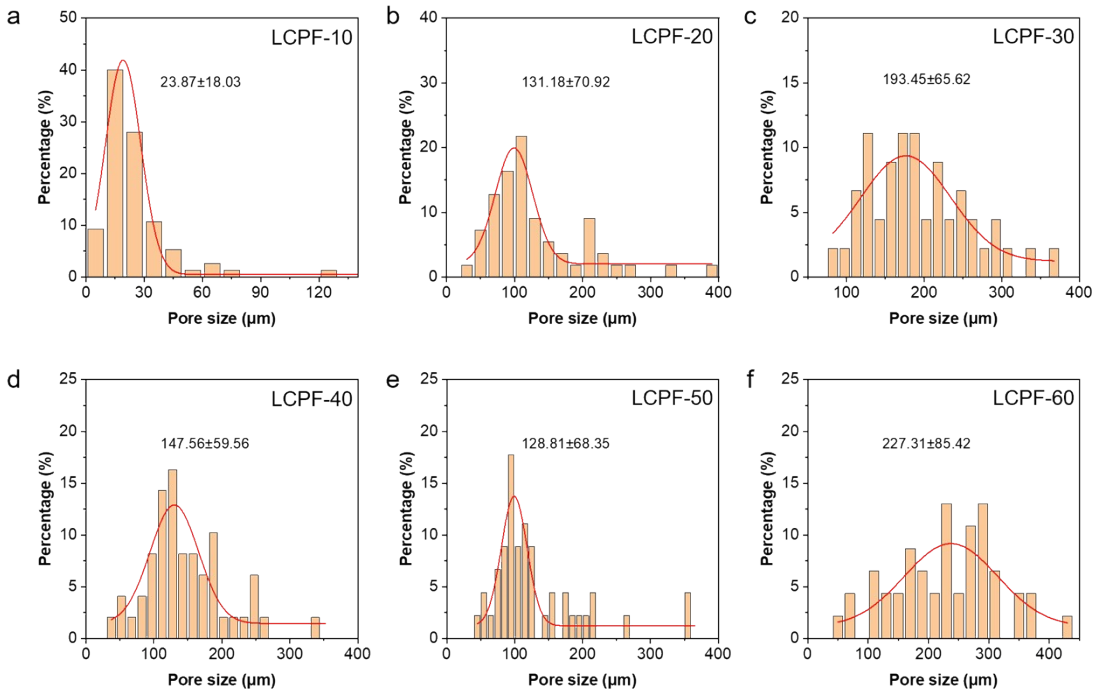

Fig. S5 Pore size distribution and mean size of the LCPFs fabricated with different solvent content: a) LCPF-10, b) LCPF-20, c) LCPF-30, d) LCPF-40, e) LCPF-50, and f) LCPF-60.

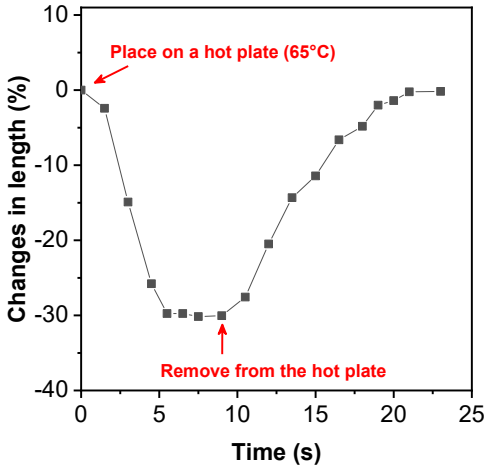

Fig. S6 Length changes of the LCEP-30 actuator during direct heating-cooling cycles using a hot plate.

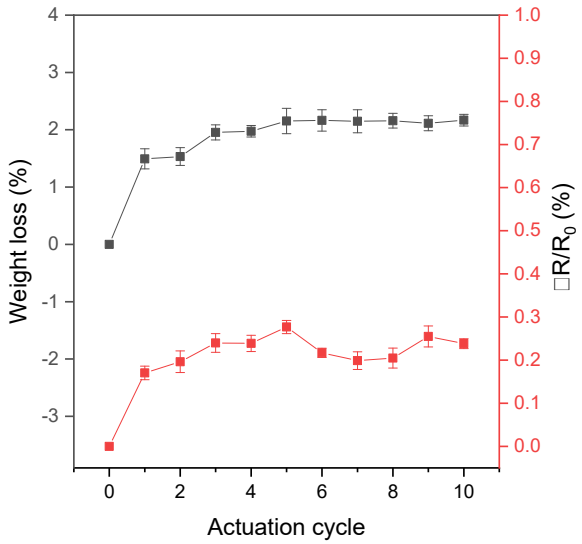

Fig. S7 Weight loss and resistance change of the LCE sensors after different actuation cycles.

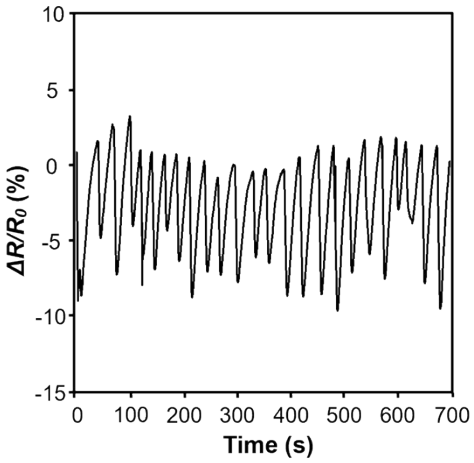

Fig. S8 Cyclic resistance change of the LCP sensors under human finger approaching and departing.

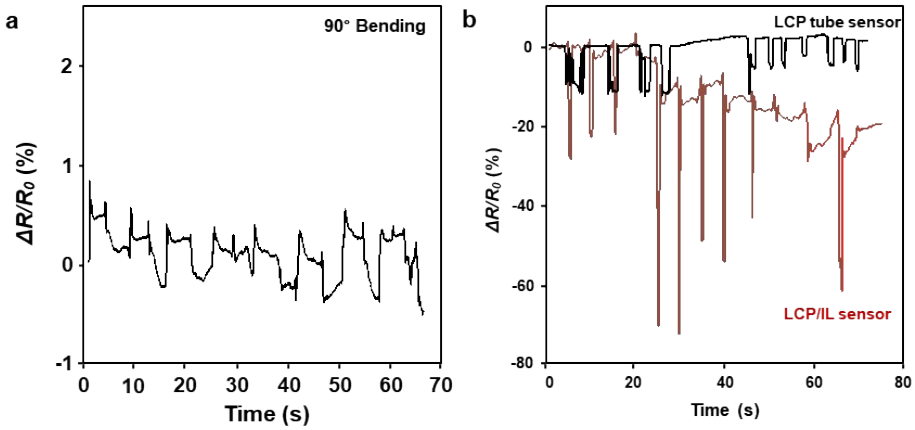

Fig. S9 Resistance changes of a) the LCPF sensor and b) the LCP tube sensor and LCP/IL sensor at bending degree of 90°.

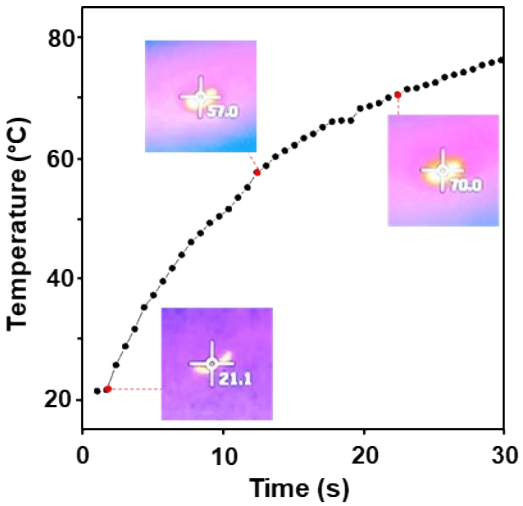

Fig. S10 Temperature change of the LCPF sensors under light.

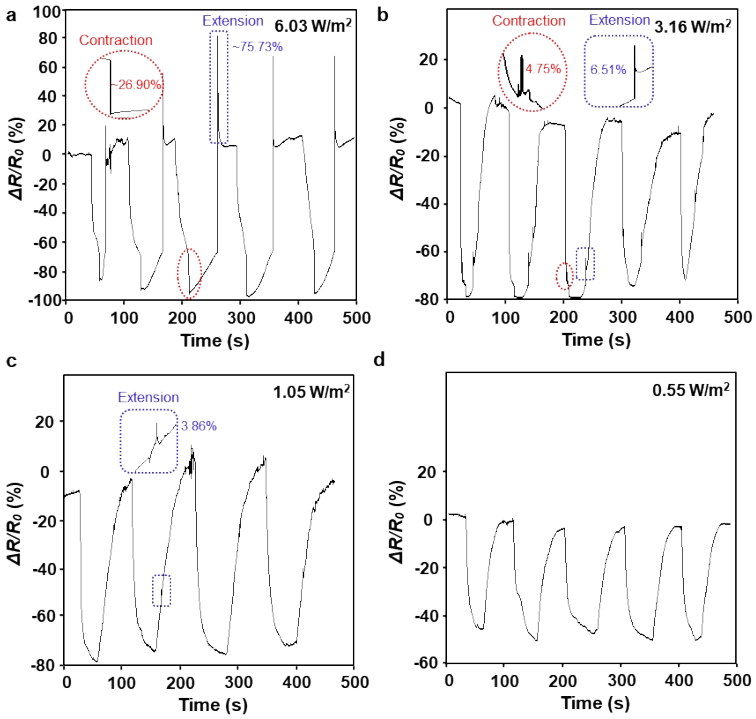

Fig. S11 Resistance changes of the LCPF sensors during heating-cooling cycles under light exposure of different intensity.

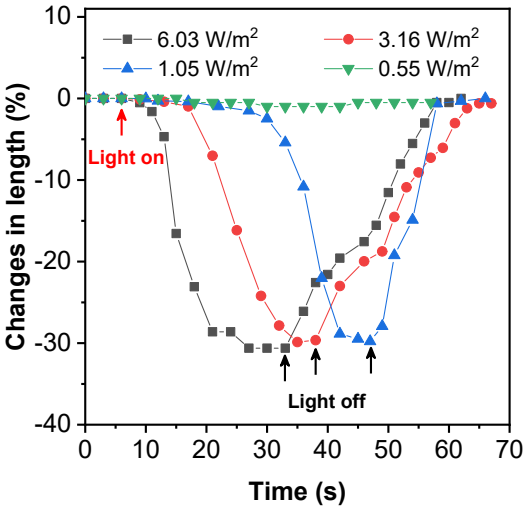

Fig. S12 Length changes of the LCEF actuator under light exposure of different intensity.

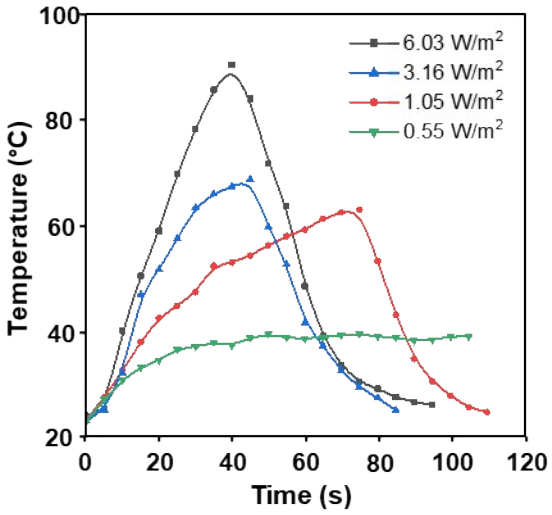

Fig. S13 Temperature changes of the LCPF sensor under light exposure of different intensity (the temperature starts to drop after turning off the light).

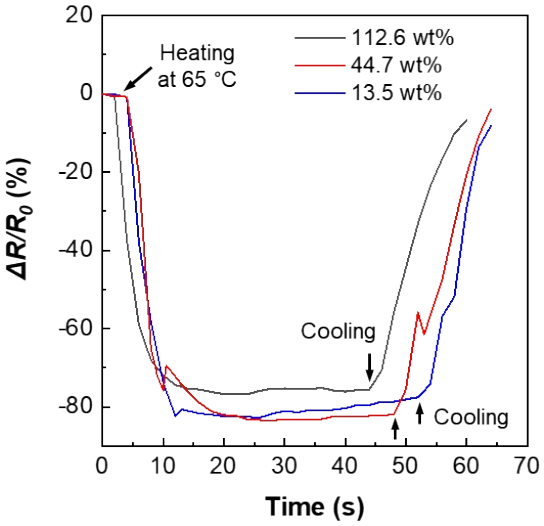

Fig. S14 Resistance changes of LCEFs incorporated with different percentage of ionic liquids.

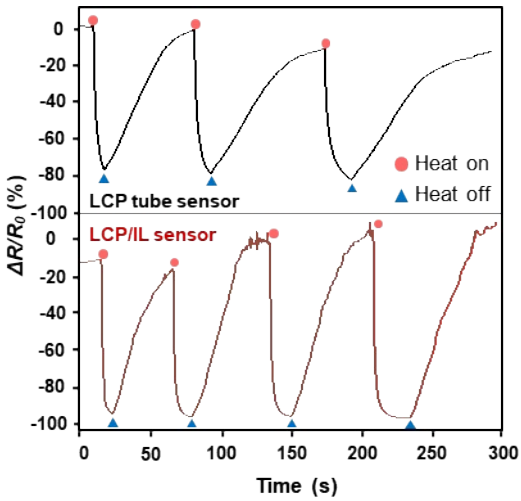

Fig. S15 Resistance change of the LCP tube sensor and LCP/IL sensor during heating-cooling cycles.

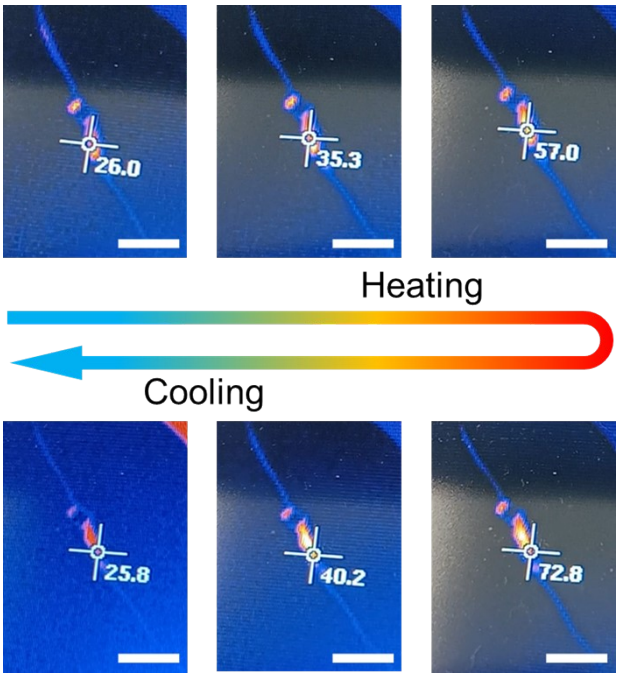

Fig. S16 Infrared images showing the temperature of the LCPF sensor during heating-cooling cycle.

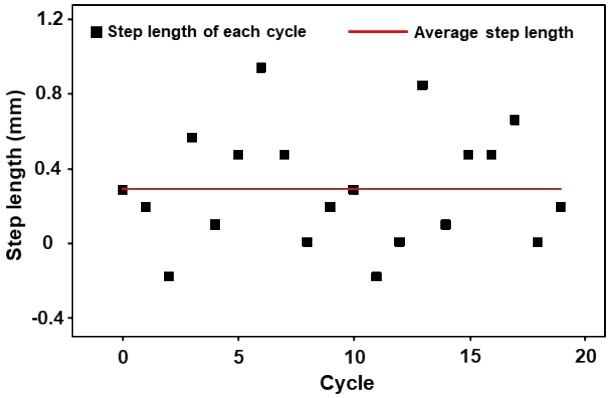

Fig. S17 Step length of the LCPF robot during actuation cycles.

Supplementary movie captions

Movie S1. Foaming process of liquid crystal polymers.
Movie S2. Light-induced actuation performance of the LCEF sensor.
Movie S3. Microstructure changes of the LCEF sensor during actuation.
Movie S4. Ultra-stable performance of the LCEF on actuation and sensing with vibration.
Movie S5. Locomotion of the LCEF-based robot.

References

1. R. Yang, L. Chen, C. Ruan, H.-Y. Zhong, Y.-Z. Wang, *J. Mater. Chem*. C **2014**, *2*, 6155-6164.
2. R. Yang, Y. Zhao, Non-uniform Optical Inscription of Actuation Domains in Liquid Crystal Polymer of Uniaxial Orientation: An Approach to Complex and Programmable Shape Changes. *Angew. Chem. Int. Ed.* **2017**, 56, 14202-14206.